Pharm Res (2020) 37: 74
https://doi.org/10.1007/s11095-020-02786-z

RESEARCH PAPER

Pre-Clinical Assessment of the Nose-to-Brain Delivery of Zonisamide After Intranasal Administration

Joana Gonçalves[1,2] • Gilberto Alves[3] • Andreia Carona[1,2] • Joana Bicker[1,2] • Carla Vitorino[4,5] • Amílcar Falcão[1,2] • Ana Fortuna[1,2]

Received: 20 November 2019 / Accepted: 17 February 2020 / Published online: 25 March 2020

ABSTRACT

Purpose Zonisamide clinical indications are expanding beyond the classic treatment of epileptic seizures to Parkinson's disease and other neurodegenerative diseases. However, the systemic safety profile of zonisamide may compromise its use as a first-line drug in any clinical condition. Since zonisamide is marketed as oral formulations, the present study aimed at exploring the potential of the intranasal route to centrally administer zonisamide, evaluating the systemic bioavailability of zonisamide and comparing its brain, lung and kidney pharmacokinetics after intranasal, oral and intravenous administrations.

Methods *In vitro* cell studies demonstrated that zonisamide and proposed thermoreversible gels did not affect the viability of RPMI 2650 or Calu-3 cells. Thereafter, male CD-1 mice were randomly administered with zonisamide by oral (80 mg/kg), intranasal or intravenous (16.7 mg/kg) route. At predefined time points, animals were sacrificed and plasma and tissues were collected to quantify zonisamide and describe its pharmacokinetics.

Results Intranasal route revealed a low absolute bioavailability (54.95%) but the highest value of the ratio between the area under the curve (AUC) between brain and plasma, suggesting lower systemic adverse events and non-inferior effects in central nervous system comparatively to intravenous and oral routes. Furthermore, drug targeting efficiency and direct transport percentage into the brain were 149.54% and 33.13%, respectively, corroborating that a significant fraction of zonisamide suffers direct nose-to-brain transport. Lung and kidney exposures obtained after intranasal administration were lower than those observed after intravenous injection.

Conclusions This pre-clinical investigation demonstrates a direct nose-to-brain delivery of zonisamide, which may be a promising strategy for the treatment of central diseases.

KEY WORDS epilepsy · intranasal · mice · nose-to-brain · pharmacokinetics · Zonisamide

ABBREVIATIONS

AUC	Area under drug concentration-time curve
AUC_t	Area under drug concentration-time curve from time zero to the time of last measurable concentration
AUC_{extrap}	Extrapolated area under drug concentration-time curve
AUC_{inf}	area under drug concentration-time curve from time zero to infinity
BBB	Blood-brain barrier
$B_{brainIN/IV}$	Brain bioavailability between IN and IV routes
C_{max}	Maximum concentration
CNS	Central nervous system
CYP	Cytochrome P450
CV	Coefficient of variation
DRE	Drug-resistant epilepsy
DTE	Drug targeting efficiency
DTP	Direct transport percentage

✉ Ana Fortuna
afortuna@ff.uc.pt; anacfortuna@gmail.com

1 Laboratory of Pharmacology, Faculty of Pharmacy, University of Coimbra, Pólo das Ciências da Saúde, Azinhaga de Santa Comba, 3000-548 Coimbra, Portugal

2 CIBIT/ICNAS - Coimbra Institute for Biomedical Imaging and Translational Research, University of Coimbra, Coimbra, Portugal

3 CICS-UBI - Health Sciences Research Centre, University of Beira Interior, Covilhã, Portugal

4 Laboratory of Technology, Faculty of Pharmacy, University of Coimbra, Coimbra, Portugal

5 Coimbra Chemistry Center, Department of Chemistry, University of Coimbra, Coimbra, Portugal

F_{Abs}	Absolute bioavailability
F_{Rel}	Relative bioavailability
HPLC	High performance liquid chromatography
IN	Intranasal
IV	Intravenous
LLOQ	Lower limit of quantification
SD	Standard deviation
SEM	Standard error of the mean
SMPA	Sulfamoylacetylphenol glucuronide
t_{max}	Time to reach the maximum concentration

INTRODUCTION

Since the beginning of the XXI century (2000–2005), zonisamide (1,2-benzisoxazole-3-methanesulfonamide) is licensed in the US and European Union for the treatment of generalized and focal seizures, not only as monotherapy in firstly diagnosed adults but also as add-on therapy in adults and children with at least 6 years old (1). Serendipitously, zonisamide also demonstrated to improve motor symptoms in patients with Parkinson's disease when co-administered with levodopa (2,3), being currently approved in Japan as adjunctive therapy of Parkinson's disease at lower doses than those used in epilepsy (4). In addition, zonisamide revealed to be effective in relieving chronic and episodic cluster headaches (5). Underlying this widespread clinical use are probably the multiple mechanisms of action of zonisamide, encompassing the blockage of voltage-dependent sodium channels and T-type calcium channels, which contribute to neural membranes stabilization (6), inhibition of carbonic anhydrase (7), alteration of dopamine metabolism (2) and reduction of glutamate release (8). Importantly, pre-clinical investigations recently highlighted that zonisamide attenuates cell death induced by seizure and/or ischemia and seems to protect the nigrostriatal dopaminergic neurons when administered to Parkinson's disease mice models (2,9). Moreover, zonisamide improved the treatment of dementia with Lewy bodies parkinsonism when it was added as an adjunct to levodopa (8).

However, in spite of its undeniable efficacy as antiepileptic drug, high potential as anti-parkinsonian drug and expected success as a neuroprotective drug in neurodegenerative pathologies, zonisamide exhibits a challenging safety profile, requiring careful patient selection and drug monitoring (10). Indeed, its safety profile is currently preventing zonisamide from being used as a first-line drug for the treatment of epilepsy or other pathological conditions (10). Among the major adverse effects of zonisamide, gastro-intestinal-related (e.g. weight loss, nauseas, dizziness) and central-related (e.g. confusion, concentration difficulty, depression, somnolence) are the most prevalent. In addition, as a carbonic anhydrase inhibitor, zonisamide commonly induces nephrolithiasis, with formation of symptomatic kidney stones (10–12). Importantly, blood concentrations of zonisamide have demonstrated to be substantially increased in patients with adverse effects than in those without adverse effects, ascribing high blood concentration as a risk factor for urolithiasis either in monotherapy or polytherapy (1,13). In this regard, the ideal administration route for zonisamide would be one that would allow the drug to attain the central nervous system (CNS) with minimal systemic exposure. However, the only currently available administration route is the oral one, which requires the systemic absorption of zonisamide followed by its passage through the blood-brain barrier (BBB) to attain the brain. Although zonisamide is completely and quickly absorbed after oral administration, reaching the maximum concentration (C_{max}) in plasma at 2–4 h, its absorption rate is slowed with concomitant food intake, while drug absorption extent remains constant (14). Moreover, zonisamide exhibits a long half-life time ($t_{1/2}$), approximately 60 h (14), which is a limitation when the drug needs to be quickly discontinued. Furthermore, the $t_{1/2}$ of zonisamide presents a high inter-individual variability and can be as low as 25 h (15,16) or as high as 80 h (10). In fact, 97% of zonisamide excretion occurs renally, 30–35% as the unchanged form, 15–20% as *N*-acetyl-zonisamide and 50% as the 2-sulfamoylacetylphenol glucuronide (SMPA), which suffers subsequently conjugation to SMAP-glucuronide (14,17). The major metabolite mainly results from the reduction of the parent compound by the cytochrome P450 (CYP) 3A4 isoform, even though CYP2C19 and CYP3A5 have also demonstrated to be involved (18). The first-pass hepatic metabolism considerably observed after oral administration not only increases inter-individual variability of its pharmacokinetic parameters particularly due to the genetic polymorphisms coupled to the CYP2C19 isoenzyme (19–21) but also the potential of zonisamide to be involved in drug-drug interactions (14). Importantly, patients co-treated with other drugs that inhibit or induce CYP3A4, are advisable to be subjected to dose adjustment, as zonisamide concentrations considerable change irrespective of the administered dose (14).

Bearing in mind the aforementioned limitations of oral formulations to deliver zonisamide into the brain, the exploitation of a novel administration route became of great interest and one of the most challenging research areas. Hence, the present research work aims at directly deliver zonisamide to the brain after intranasal administration, thereby reducing drug systemic exposure and ameliorating its safety profile. Non-invasive nose-to-brain drug transport via olfactory epithelium has revealed to be a promising strategy for chronically given central-acting drugs with potential increasing of patient compliance (22–27). For instance, we have demonstrated that the antiepileptic drug, levetiracetam, loaded in a thermorreversible gel composed of Carbopol 974P, achieved higher concentrations in the brain 5 min after

intranasal administration than after administration by classic systemic route (23). In theory, it has been postulated that drugs can be transported from the nasal cavity directly to cerebrospinal fluid (CSF) or brain parenchyma through two possible routes along the olfactory neurons: the olfactory nerve pathway (intracellular axonal transport) and the olfactory epithelial pathway (extracellular perineural transport). The extracellular transport, apparently a faster route of nose-to-brain delivery, allows drugs to paracelullarly cross the perineural epithelium into the fluid-filled perineuronal space (within 30 min), mainly by a bulk flow transport phenomenon, along the olfactory axon up to the subarachnoid space filled with CSF. On the other hand, the intracellular mechanism has been proposed as a feasible route to transfer drugs directly to the brain via intracellular axonal transport along the olfactory sensory neurons. Accordingly, there is a slow axonal internalization of the molecule (endocytosis) and subsequent release by exocytosis into the olfactory bulb and other brain areas by the anterograde axoplasmic flow (28). Nevertheless, due to the physiological defense mechanisms of nasal mucosa, compounds administered in nasal cavity often suffer mucocilliary clearance and are quickly eliminated from the nasal mucosa. This hampers the drug to remain enough time in olfactory epithelium, compromising its distribution into the brain (29).

Therefore, for the first time, the present study characterized the pharmacokinetics of zonisamide in plasma, brain, lung and kidney after intranasal (IN) administration, comparing them to those observed after oral and intravenous (IV) administrations. Due to the aforementioned principle and advantages of IN delivery route, the present study made use of a mucoadhesive formulation to reduce the clearance rate of zonisamide and increase its delivery into the brain.

MATERIAL AND METHODS

Chemicals and Reagents

Zonisamide was acquired from Molekula SRL (Rimini, Italy) while antipyrine and pluronic F-127 were obtained from Sigma-Aldrich (St. Louis, MO, USA) and Carbopol 974P and Noveon® Polycarbophil were kindly provided by Lubrizol (Wickliffe, OH, USA). Quantification of zonisamide in pharmacokinetic study samples required acetonitrile of High Performance Liquid Chromatography (HPLC) gradient grade (Fisher Scientific, Leicestershire, UK) and ultrapure water (HPLC grade, 18.2 MΩ.cm), which was prepared using a Milli-Q water apparatus from Millipore (Milford, MA, USA). Reagents used for sample homogenization and drug extraction included hydrochloric acid fuming 37%, disodium hydrogen phosphate dihydrate and sodium dihydrogen phosphate dihydrate, from Merck KGaA (Darmstadt, Germany), and dimethyl sulfoxide (DMSO), ethyl acetate and methanol from Fisher Scientific (Leicestershire, UK). Animals were anesthetized with ketamine (Imalgene 1000®, 100 mg/ml) and xylazine (Vetaxilaze 20®, 20 mg/ml), both commercially available. All the remaining chemicals and reagents were obtained from Sigma-Aldrich (St. Louis, MO, USA) unless otherwise specified.

In Vitro Assays

Human Lung Adenocarcinoma Cell Line In Vitro Viability

The viability of human lung adenocarcinoma cells (Calu-3, ATCC® HTB-55TM) was tested by exposing them to zonisamide at various concentrations. Dulbecco's modified Eagle's medium (DMEM, Sigma-Aldrich) with 0.04 M sodium bicarbonate and enriched with inactivated fetal bovine serum (10%, *v/v*) and penicillin-streptomycin (1%, *v/v*) was used as culture medium for Calu-3 cells. These cells were grown in T-75 flasks (Orange-Scientific, Braine-l'Alleud, Belgium), passaged 3 times/week using a 0.25% Trypsin-EDTA solution and cultured at 37°C in 95% relative humidity and 5% CO_2.

The viability of Calu-3 cells was determined applying the Alamar Blue assay, performed in accordance with (30). Briefly, cells were seeded in 96-well plates (3.5×10^4 cells/well) and incubated for 24 h at 37°C and 5% CO_2. After removing the culture medium, control cell group was put into contact with fresh medium without zonisamide, while the treatment groups were incubated with zonisamide at the following concentrations: 1, 5, 10, 25, 50 and 100 μM. The incubation treatment time was 24 h. Afterwards, treatment solutions were withdrawn and fresh medium with 10% Alamar Blue solution (125 mg/mL) was added to each well. After an incubation of 3 h, fluorescence was measured (560 nm / 590 nm) on the Biotek Synergy HT microplate reader (Biotek Instruments®, Winooski, VT, USA).

The Alamar Blue assay is based on the quantification of resorufin, a substance with endogenous fluorescence and that results from the reduction of resazurin by viable cells. The viability of the cells was determined in accordance with the following equation:

$$Cell\ viability\ (\%) = \frac{FL_T - FL_W}{FL_{Control} - FL_W} \times 100 \quad (1)$$

FL refers to the mean value of fluorescence displayed after incubation with the treatment solution (FL_T), in the controls ($FL_{control}$) and in the wells without cells (FL_W).

Human Nasal Septum Cell Line Cell Line In Vitro Viability

The human nasal septum cell line (RPMI-2650, ECACC 88031602) was used to evaluate the influence of zonisamide

and both gels on cell viability and, hence, select the most suitable formulation to be administered to mice.

The culture medium used for RPMI-2650 cells was the Minimum Essential Medium Eagle (EMEM) with Earle's salts and sodium bicarbonate, and enriched with glutamine (2 mM), nonessential amino acids (1%, *v/v)*, heat-inactivated fetal bovine serum (10%, *v/v*) and penicillin-streptomycin mixture (1%, *v/v*). Grown conditions were those aforementioned for Calu-3 cell line.

After optimization of the protocol, Alamar Blue assay was performed as described in section "In Vitro Cell Viability Studies", with the exception of cell density, which was 3.0×10^5 cells/well, and the period of incubation with Alamar Blue solution which was only 2 h. The differences of incubation period and cell density were defined according to the metabolizing capacity of the cells. Metabolically viable cells convert non-fluorescent resazurin (Alamar Blue) into highly fluorescent resorufin. Thus, cell lines with higher metabolic activity require a shorter incubation time. The experimental conditions herein tested included: zonisamide in concentrations ranging from 1 to 100 μM; Noveon® Polycarbophil or Carbopol® 974P gels unloaded; and both gels loaded with zonisamide at the concentrations of 50, 100, 150, 200, 250 and 400 μM.

In Vivo Pre-Clinical Studies

Ethical Considerations and Animals

The European Directive (2010) regarding the protection of laboratory animals used for scientific purposes (2010/63/EU) (European Parliament, Council of the European Union, 2010) and the Portuguese law on animal welfare (Decreto-Lei 113/2013) were taken into account when designing and performing these investigations. In addition, the studies were authorized by the national entity, *Direção-Geral de Alimentação e Veterinária (DGAV*, 421/000/000/2016*)*, and all efforts were made to reduce the number of used animals and their suffering.

The pre-clinical studies were carried on adult male CD-1 mice weighing between 25 and 30 g. They were acquired to Charles River Laboratories (France) and acclimatized to the local bioterium for at least 1 week. During this period, animals were housed in groups of five animals at controlled environmental conditions (20 ± 2°C; relative humidity 55 ± 5%; 12 h light/dark cycle). Standard rodent diet (4RF21, Mucedola®, Italy) and tap water were of ad libitum access during acclimatization and all experimental procedures.

Preparation of Zonisamide Formulations

For IN administration, the appropriate amount of zonisamide was firstly dissolved in DMSO to obtain the final concentration of 400 mg/mL; 25 μL of this stock solution was added to 975 μL of the thermoreversible gel, yielding a final zonisamide concentration of 10 mg/mL. Briefly, Pluronic f-127 (18% *w/v*) was dissolved in 10 mL of cold Milli-Q water and stored at 4°C overnight for complete hydration of the flakes. Subsequently, 0.02 g of Carbopol® 974P or the same amount of Noveon® Polycarbophil was added until complete dissolution as described in (23). The gel was selected according to the results obtained during *in vitro* tests (section "In Vitro Cell Viability Studies"), with Carbopol® 974P being the polymer for which the results were more favorable.

In order to obtain an adequate IV solution (without suspension particles), different solvents were tested to prepare a concentrated stock solution of zonisamide. Transcutol® (Diethylene Glycol Monoethyl Ether) was selected, as it allowed zonisamide to solubilize at 10 mg/mL. This solution was, then, diluted in sodium chloride 0.9% solution (B. Braun Medical, Queluz de Baixo, Portugal) to attain the final concentration of 4.17 mg/mL without compromising physiological pH and fluidity.

For oral administration, zonisamide was suspended in sodium chloride 0.9% solution at the final concentration of 3.2 mg/mL.

In Vivo Pharmacokinetic Study

Pharmacokinetic studies were performed to compare the pharmacokinetics of zonisamide in different biological matrices after its single-dose administration by IN, IV and oral routes.

To attain this objective, 140 animals were randomly divided into three groups: 45 animals received zonisamide by IN route, 50 by oral route and 45 by IV. All animal groups were pre-anesthetized with ketamine/xylazine (100/10 mg/kg, intraperitoneal) and kept in a heated environment to avoid hypothermia.

Regarding the IN administered animal group, 50 μL of the thermoreversible gel loaded with zonisamide, corresponding to 16.7 mg/kg, were aerosolized using the high pressure system MicroSprayer® Aerosolizer (model IA-1B, Penn-Century, Inc., Wyndmoor, PA) connected to a high pressure syringe (Model FMJ-250 from Penn-μCentury, Inc., Wyndmoor, PA). The device was introduced approximately 1 mm into the left nostril of anesthetized mice, while anatomically positioned in right lateral decubitus.

The same dose reported for the IN route was administered intravenously via the injection of 120 μL of the previously prepared solution with final concentration of 4.17 mg/mL. Both IN and IV administered animal groups were sacrificed at 5, 15, 30, 60, 90, 120, 240, 360 and 480 min post-administration (5 animals per time point).The group of orally treated animals was also previously anesthetized, in order to mimic the conditions of IN and IV groups. The administered single dose was 80 mg/kg and sample collection times were 5, 15, 30, 60, 90, 120, 240, 360, 480 and 780 min post-administration.

The animals were sacrificed at the defined endpoints by cervical dislocation and decapitation. Blood was quickly collected to heparinized tubes, centrifuged at 2880 g (4°C, 10 min) to obtain plasma while the tissues were excised, cleaned with sodium chloride 0.9% solution, weighted and homogenized with 0.1 M sodium phosphate buffer pH 5.0 (4 mL/g) by use of the THOMAS® Teflon. Homogenates were also centrifuged at 2880 *g* (4°C, 15 min) and, similarly to plasma, the supernatant samples were collected and kept frozen at −80°C until preparation and analysis by HPLC.

Drug Analysis

Before quantitative analysis, both plasma (100 μL) and tissue supernatants (150 μL) were spiked with the internal standard (antipyrine, 50 μg/mL) and, then, subjected to protein precipitation with methanol and two liquid-liquid extractions with ethyl acetate in order to remove endogenous contaminants and extract zonisamide. More details of extraction and concentration procedures can be found in (23).

To quantify zonisamide in the biological samples collected from *in vivo* pharmacokinetic studies, 20 μL of each final prepared sample was injected into the Shimadzu HPLC system (Shimadzu Corporation, Kyoto, Japan) composed of LC-20A solvent delivery model, DGU-20A5 degasser system, SIL-20AHT auosampler, CTO-10ASVP column oven (set at 40°C) and SPD-M20A diode array detector (used at 220 nm and 239 nm for antypirin and zonisamide, respectively). LCsolution software (Shimadzu Corporation, Kyoto, Japan) controlled HPLC apparatus and data acquisition. Chromatographic separation was achieved on a LiChroCART® Purospher® Star C_{18} reverse phase column (55 × 4 mm, 3 μm; Merck KGaA, Darmstadt, Germany) and using a mobile phase of water and acetonitrile with gradient elution, based on our previously validated method (31).

Before analyzing the samples, the bioanalytical method was partially validated considering the guidelines defined by the European Medicines Agency (32,33) and Food and Drug Administration (34) as demonstrated in Table I and Fig. 1.

Pharmacokinetic Analysis and Statistical Analysis

The maximum concentrations (C_{max}) and respective times to reach peak concentrations (t_{max}) of zonisamide in plasma and tissues were directly estimated in accordance with the temporal evolution of drug concentrations. The other pharmacokinetic parameters that were herein estimated included two related with drug exposure – the area under the curve (AUC) from time zero to the last time with quantifiable concentration (AUC_t), from time zero to infinity (AUC_{inf}) [determined by calculating $AUC_t + (C_{last/kel})$, where C_{last} is the last quantifiable concentration and k_{el} is the apparent elimination rate constant] – and other two related with drug elimination – $t_{1/2}$ and the mean residence time (MRT). The $t_{1/2}$ was estimated as the quotient of ln2 per k_{el}, while MRT represents the average time a molecule stays in the body and is estimated as the ratio between the area under the first moment curve or the curve of concentration versus time and the correspondent AUC. All the aforementioned pharmacokinetic parameters were estimated by non-compartmental analysis, using the WinNonlin version 5.2 (Pharsight Co, Mountain View, CA, USA). Non-compartmental analysis was herein selected because it considers the mean concentrations ($n = 5$) obtained at each endpoint without assuming an exponential function and, consequently, decreasing the bias of the estimated pharmacokinetic parameters. In addition, the extrapolated area under the curve (AUC_{extrap}) was calculated in percentage, corresponding to the percentage of AUC extrapolated from t_{last} to infinity. This is a relevant parameter, since AUC_{extrap} should preferably be inferior to 20% to guarantee that samples were collected during enough time to accurately describe zonisamide's pharmacokinetics.

The absolute and relative bioavailabilities were estimated according to Eqs. 2 and 3, respectively:

$$F_{Abs} = \frac{AUC_{infIN} \times Dose_{IN}}{AUC_{infIV} \times Dose_{IV}} \times 100 \quad (2)$$

$$F_{Rel} = \frac{AUC_{infIN} \times Dose_{IN}}{AUC_{infOral} \times Dose_{Oral}} \times 100 \quad (3)$$

where AUC_{infIN}, AUC_{infIV} and $AUC_{infOral}$ are the AUC_{inf} values observed following IN, IV and oral administration, respectively; $Dose_{IV}$, $Dose_{IN}$ and $Dose_{Oral}$ represent the drug dose (mg/kg) administered by IV, IN and oral routes.

The ratio between AUC_{tissue} and AUC_{plasma} was calculated for each tissue sample collected from three animal groups in order to assess drug distribution into the three tissues under analysis and verify whether it depends on the administration route.

In addition, the percentage efficiency of drug targeting (DTE) and the percentage of direct transport (DTP) were calculated following Eqs. 4 and 5, respectively.

$$DTE\ (\%) = \frac{\left(AUC_{brain}/AUC_{plasma}\right)_{IN}}{\left(AUC_{brain}/AUC_{plasma}\right)_{IV}} \times 100. \quad (4)$$

$$DTP\ (\%) = \frac{AUC_{brain\ IN} - \left[\frac{AUC_{brain\ IV}}{AUC_{plasma\ IV}} \text{ x } AUC_{plasma\ IN}\right]}{AUC_{brain\ IN}} \times 100 \quad (5)$$

where AUC_{plasma} and AUC_{brain} correspond to the AUC_t observed in plasma and brain, respectively. According to

Table I Main parameters of the HPLC-DAD method validation employed to quantify zonisamide in plasma, brain, lung and kidney matrices ($n = 5$)

Validation Parameter	Plasma	Brain	Lungs	Kidneys
Calibration range[a] (μg/mL)	0.5–50	0.2 – 200[b]	0.2–200 [b]	4–200 [b]
Regression Equation[a]	y = 0.0566658x - 0.010688	y = 0.095754x + 0.008597	y = 0.116435x - 0.057024	y = 0.119375x - 0.045099
Coefficient of determination (r^2)	0.9958	0.9918	0.9949	0.9950
LLOQ (μg/mL)	0.5	0.2 [b]	0.2 [b]	4 [b]
Inter-day				
Precision (%CV)	2.88–9.48	4.27–12.24	3.23–7.34	9.57–10.86
Accuracy (%Bias)	−1.52 – 13.42	−13.74 – 2.95	0.70–2.15	−10.16 – 9.87
Intra-day				
Precision (%CV)	2.81–9.91	5.36–7.66	1.89–5.20	2.87–7.96
Accuracy (%Bias)	0.60–8.88	−5.30 – 2.10	2.59–7.46	−1.04 – 1.50
Recovery (%)	68.38–81.45	69.10–87.07	64.47–84.59	65.93–90.46

[a] Inter-day values, n = 5; [b] values expressed in μg/g

LLOQ, lower limit of quantification; CV, coefficient of variation; Bias, deviation from nominal value

literature, it is established that transport is preferential to the brain compared to the systemic pathway, when DTE is greater than 100% (35–37). On the other hand, DTP estimate the drug percentage that directly attained the brain after administration into the nasal cavity, without involving systemic absorption followed by the passage through the BBB. Thus, DTP values greater than 0 indicate direct drug targeting, so the lower plasma and brain exposure following IV administration, the greater the amount of drug that reaches the brain by direct transport (38). Even though both DTE and DTP have been associated to be high variable depending on the in vivo protocols (39), they were herein chosen as they are the most mentioned parameters to assess nose-to-brain delivery and to compare different routes of administration (40).

The brain bioavailability of the drug has also been estimated to evaluate which pathway allows greater drug accumulation at the therapeutic target, according to the quotient:

$$B_{\text{brain IN/IV}} = \frac{AUC_{\text{brain IN}}}{AUC_{\text{brain IV}}} \quad (6)$$

Statistical Analysis

Graphpad Prism® 5.03 (San Diego, CA, USA) was used to construct graphics and perform the statistical data both from the in vitro cell investigations and in vivo pharmacokinetic study. The in vitro results were expressed as mean ± standard deviation (SD) and ANOVA test was used to determine differences of cell viability (%) after incubation with zonisamide/formulations compared with untreated control cells (100% cell viability). On the other hand, in vivo pharmacokinetic data was expressed as mean ± standard error of the mean (SEM) and the two-way ANOVA test followed by the Dunnett's multiple comparison test were applied to determine statistical differences among the three administration routes of administration (dose-normalized concentrations versus time).

In both data types, differences were considered statistically significant when p-values were inferior to 0.05 ($p < 0.05$).

RESULTS

In Vitro Cell Viability Studies

The results found for Alamar Blue assay (Fig. 2) demonstrated no decrease on the viability of the Calu-3 and RPMI-2650 cells in the presence of zonisamide for 24 h at the tested concentrations (1–100 μM), since no statistically significant differences were observed compared to the negative control. Indeed, cell viability was within ±15% compared with negative control, which is acceptable by international guidelines.

As described in section "Preparation of Zonisamide Formulations", two thermorreversible gels were herein tested: one encompassing 0.02 g of Carbopol® 974P while the other integrated the same quantity of Noveon® Polycarbophil. The viability of RMPI 2650 cells was screened in the presence of these two gels. Empty or loaded with zonisamide, the gels did not impair cell viability within the range of 50 to 400 μM (Fig. 3). Nevertheless, it is noteworthy that the Noveon® polycarbophilic gel loading zonisamide revealed lower cell viability (ranging from 82.78 to 94.46%) when compared to the zonisamide-loaded Carbopol® 974P gel (ranging from 99.32 to 105.16%). For this reason, the thermoreversible gel prepared with Carbopol® 974P was selected to be administered to mice.

Pharmacokinetics of Zonisamide

Mean concentration-time profiles ($n = 5$) of zonisamide in plasma, brain, lung and kidney obtained after administration

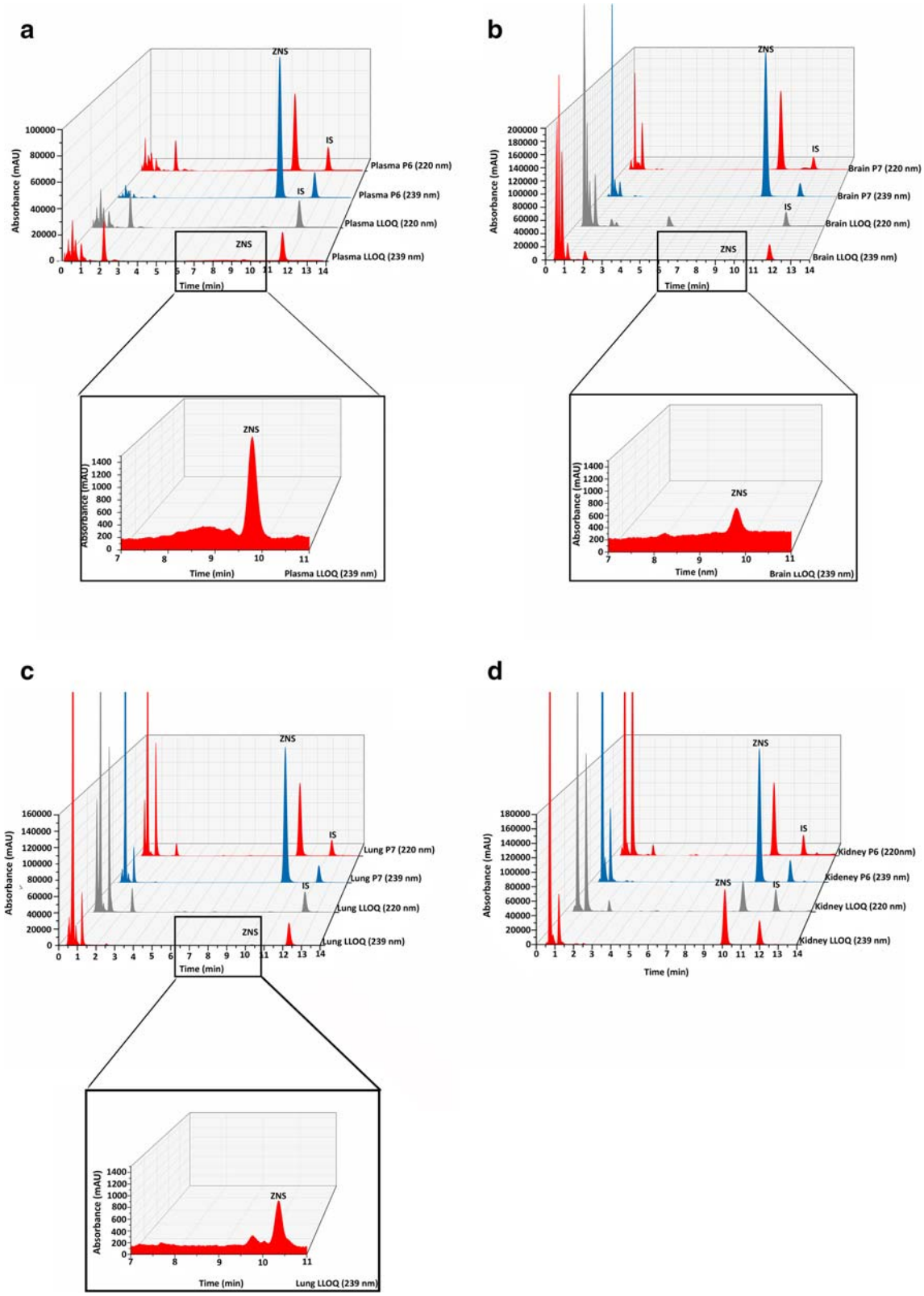

Fig. 1 – Representative chromatograms achieved during validation of the analytical technique described in section "Drug Analysis" for mice plasma (A), brain (B), lung (C) and kidney (D) spiked at the lower limit of quantification (LLOQ) level and at the upper limit of quantification (ULOQ) of the calibration ranges; the internal standard (IS, antypirine) was detected at 220 nm while zonisamide was at 239 nm

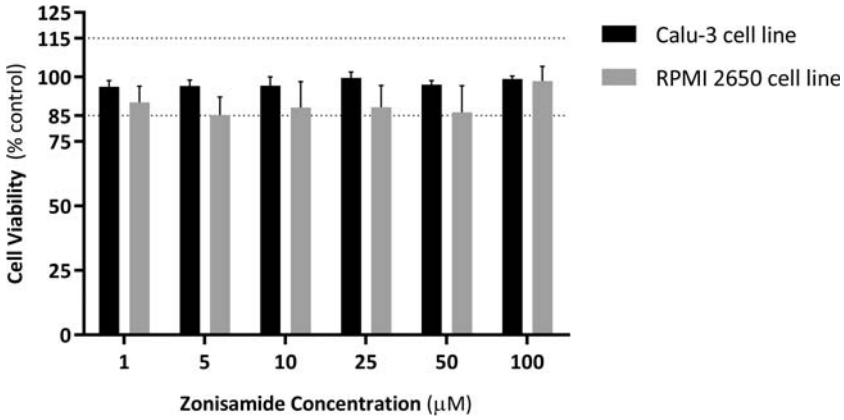

Fig. 2 – Viability (%) of Calu-3 and RPMI 2650 cells after incubation with zonisamide for 24 h (1, 5 10, 25, 50 and 100 μM). Data represented as mean ± standard deviation ($n = 4$, three independent replicates)

of one dose of IV solution (16.7 mg/kg), IN thermoreversible *in situ* gel (16.7 mg/kg) or oral suspension (80 mg/kg) to mice are presented in Fig. 4. Since the administered oral dose was different from the IV and nasal ones, zonisamide concentrations were normalized according to the administered drug dose of the corresponding route (Fig. 5)-, the Dunnett's multiple comparison test results obtained for oral and IN routes using IV as the control comparator are also depicted in Fig. 5. The corresponding mean pharmacokinetic parameters of zonisamide in plasma, brain, lung and kidney are summarized in Table II and the dose-normalized pharmacokinetic parameters in Table III.

Regarding plasma levels, zonisamide concentrations achieved after IN administration were lower than those observed after IV and oral routes, at all the collected time-points (Fig. 4A). Identically to IV route, IN delivery allowed zonisamide to attain the mean C_{max} in plasma at 5 min post-dosing (Table II). Furthermore, after IN dosing, zonisamide exhibited the lowest value of C_{max} (9.93 μg/mL versus 13.72 and 31.33 μg/mL observed for IV and oral routes, respectively) and AUC_t (1832.63 μg.min/mL versus 3955.13 and 3813.40 μg.min/mL for IV and oral routes, respectively). As these results were found with IN and IV doses that were 4.79-fold lower than the oral dose (16.7 mg/kg and 80 mg/kg, respectively), the lower plasma exposure of zonisamide is undeniable after IN delivery (as corroborated by the IN absolute bioavailability of 54.95%). In addition, comparing the dose-normalized plasma AUC_t following IN and IV administrations, an increment of approximately 2.16-fold is detected for the IN route, confirming the advantage of its lower systemic exposure (Table III). In opposition, the AUC_t/dose obtained after oral administration was 2.30-fold lower than the one of IN route. Nevertheless, in brain tissue, the AUC_t/dose observed after oral route was 2.44-fold lower than that after IN route, suggesting a decreased brain-target delivery when orally administered. Indeed, observing Fig. 4B-D, it is noteworthy that the concentrations achieved in brain, liver and kidney tissues are considerably higher for oral route at almost all time-points. This is not surprising, since the oral dose was considerably higher than IV or IN doses, confirming the importance of analyzing dose-normalized concentrations depicted in Fig. 5, when comparing with oral route. Accordingly, zonisamide concentrations presented the smallest values after oral administration in all tissues.

When comparing brain concentration-time profiles after IV and IN administration (Fig. 4B), it is particularly interesting to observe the anticipation of t_{max} of IN zonisamide in relation to IV formulation (120 min versus 240 min, Table II). In addition, it is noteworthy that, at 5 min post-IN-dosing, zonisamide concentration is significantly increased relatively to the

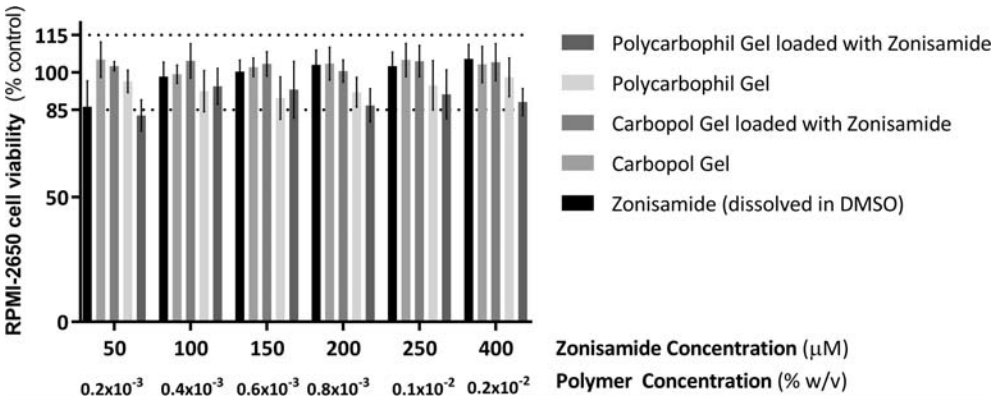

Fig. 3 – Viability (%) of RPMI-2650 cells after incubation with zonisamide for 24 h (50–400 μM); empty Noveon® Polycarbophil and Carbopol® (0.02% for both) thermoreversible gels; and thermoreversible gels loaded with zonisamide at the same concentrations. Data represented as mean ± standard deviation ($n = 4$, three independent replicates)

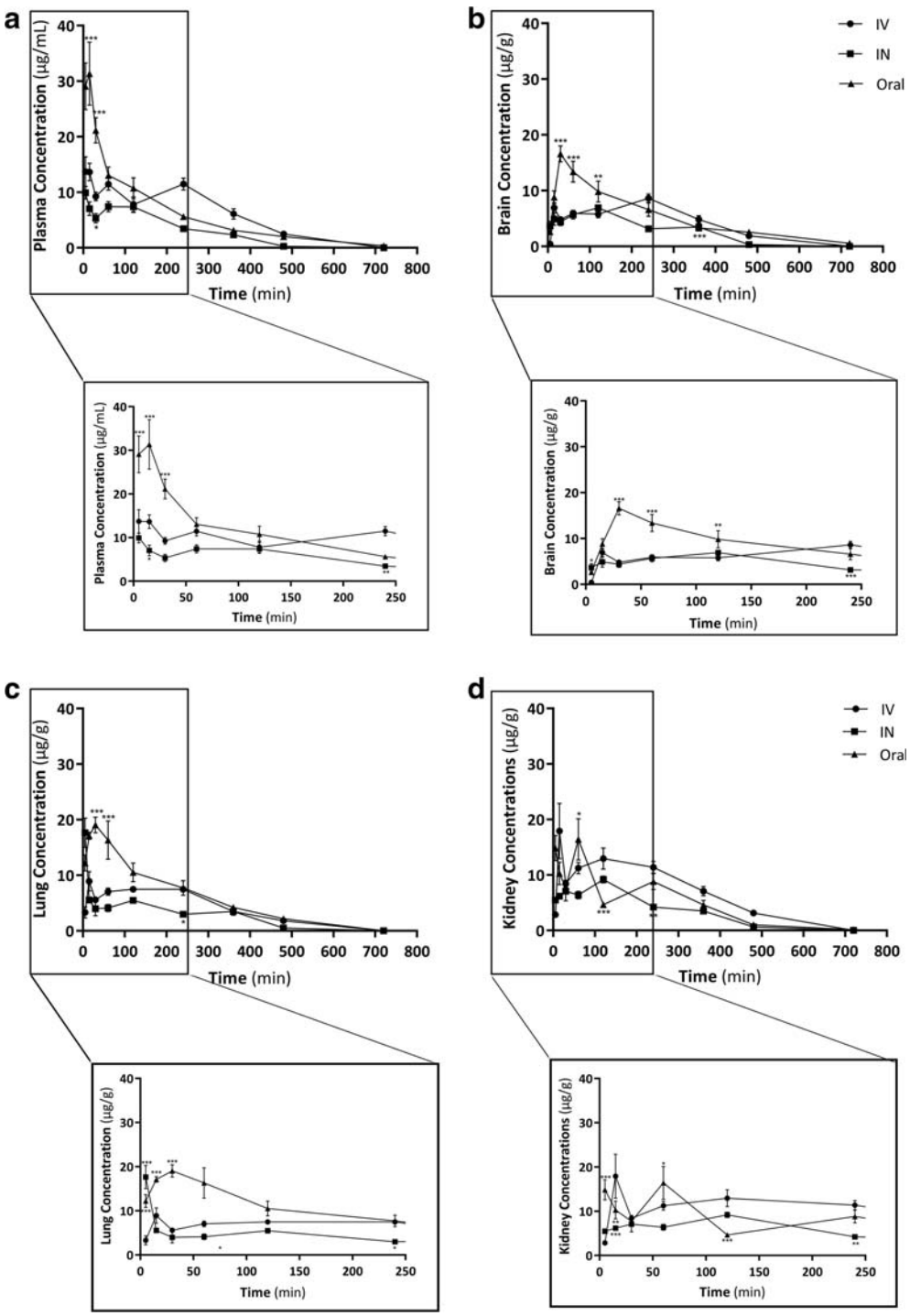

Fig. 4 – Concentration-time profiles of zonisamide up to 800 min post-dosing in plasma (A), brain (B), lung (C) and kidney (D) following intranasal (IN, 16.7 mg/kg), intravenous (IV, 16.7 mg/kg) or oral administration (80 mg/kg) to mice. The figure bellow each profile corresponds to the respective enlargement up to 250 min post-administration. Symbols represent the mean values ± SEM of five determinations per time point ($n = 5$)

IV injection (3.636 ± 0.867 and 0.420 ± 0.075 µg/g, respectively), presenting a p value of 0.021. Statistical differences were not identified at other time-points, with the exception of 240 min, when concentrations were considerably lower for IN route [11.470 versus 3.437 µg/g, respectively; $p = 0.0065$, which is in accordance with the superior k_{el} of zonisamide after IN administration than IV injection (Table II). Moreover, plasma concentration-time profiles traced for both administration routes, revealed statistical differences, not at 5 min, but at 15 min $p = 0.0087$; t (4) = 4.797] and 240 min $p = 0.0020$; t (4) = 7.218] post-administration, suggesting that, at 5 min, an additional route allowed zonisamide to reach the brain tissue besides the systemic one. Consistently, DTE was 149.54% and DTP was 33.13%. Furthermore, at 5, 15 and 30 min post-administration, the highest brain-to-plasma ratios were observed after IN administration, exhibiting significant

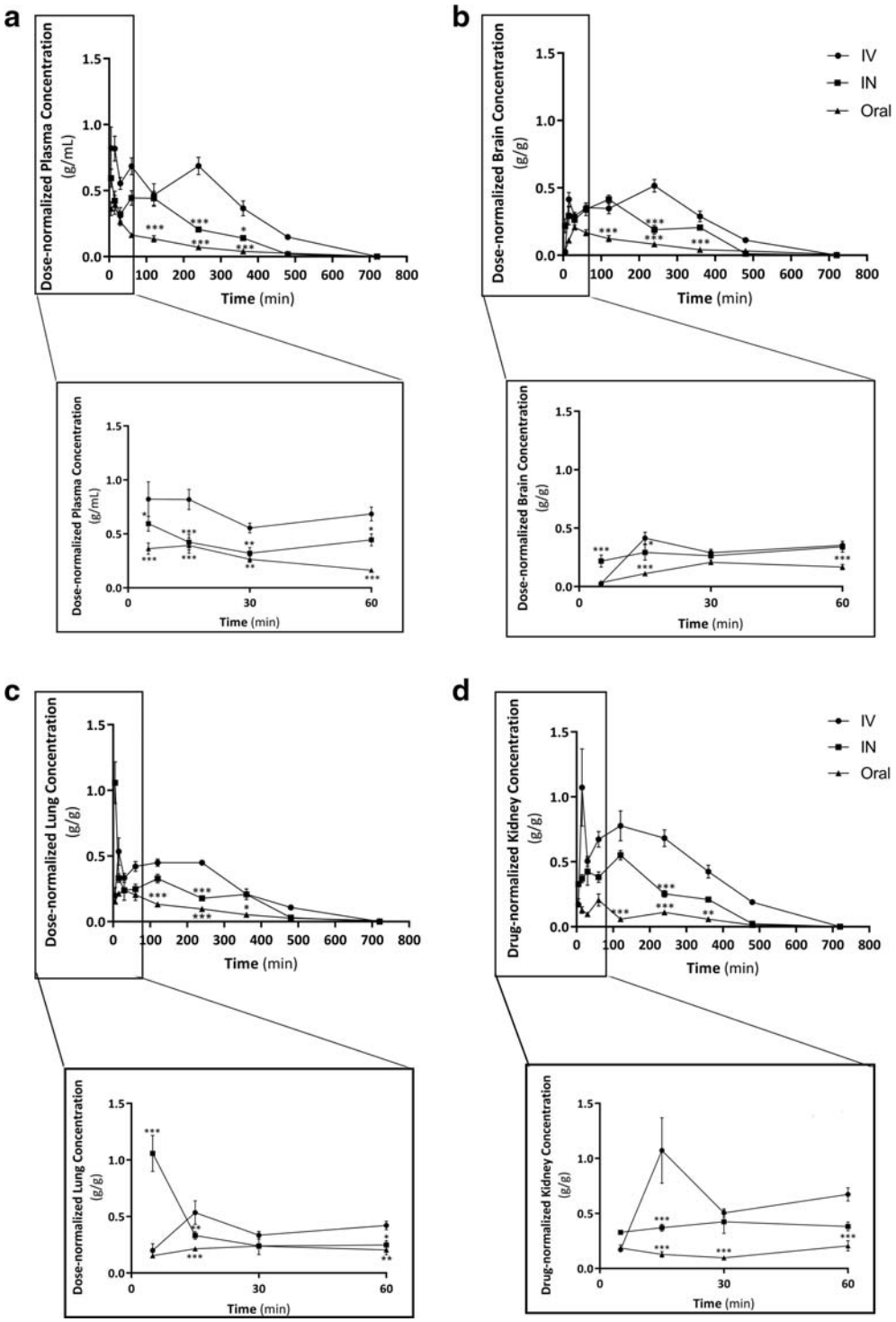

Fig. 5 – Dose-normalized concentration-time profiles of zonisamide up to 800 min post-dosing in plasma (**A**), brain (**B**), lung (**C**) and kidney (**D**) following intranasal (IN, 16.7 mg/kg), intravenous (IV, 16.7 mg/kg) or oral administration (80 mg/kg) to mice. The figure bellow each profile corresponds to the respective enlargement up to 60 min post-administration. Symbols represent the mean values ± SEM of five determinations per time point ($n = 5$). Statistical differences are in relation to the IV administration route as follows: $^{*}p < 0.05$, $^{**}p < 0.01$, $^{***}p < 0.001$ assessed by two-way ANOVA followed by Dunnett's multiple comparison test

statistical differences relatively to IV and oral routes, as detailed in Fig. 6A. In opposition, from 60 to 480 min, evolution of brain-to-plasma ratios after administration of the thermoreversible gel is parallel to that observed after IV injection, demonstrating that zonisamide attained the brain after systemic absorption and BBB crossing.

Since intranasally administered drugs may reach the lungs in mice, which may compromise the safety of the zonisamide IN formulation, lung tissue was also analyzed in the present study. From Fig. 4C and Table II, it is undeniable that, in lungs, the IN route was the fastest to attain the C_{max}, which was almost twice of that observed after IV injection (17.66

Table II Pharmacokinetic parameters of zonisamide in plasma, brain, lung and kidney tissues following its intranasal (IN, 16.7 mg/kg), intravenous (IV, 16.7 mg/kg) and oral (80 mg/kg) administration to mice

Pharmacokinetic Parameters[a]	Plasma			Brain			Lung			Kidney		
	IV	IN	Oral	IV	IN	Oral	IV	IN	Oral	IV	IN	Oral
t_{max} (min)	5.00	5.00	15.00	240.00	120.00	30.00	15.00	5.00	30.00	15.00	120.00	60.00
C_{max} (μg/mL)	13.72	9.93	31.33	8.61[b]	6.91[b]	16.60[b]	8.93[b]	17.66[b]	19.04[b]	17.90[b]	9.19[b]	16.42[b]
AUC_t (μg.min/mL)	3955.13	1832.63	3813.40	2708.61[c]	1876.78[c]	3691.84[c]	2680.70[c]	1794.50[c]	4315.82[c]	4515.67[c]	2358.06[c]	3245.41[c]
AUC_{inf} (μg.min/mL)	4342.48	2386.23	4248.20	3003.11[c]	1920.93[c]	3804.93[c]	2984.67[c]	1980.00[c]	4435.77[c]	5104.55[c]	2453.99[c]	3358.92[c]
AUC_{extrap} (%)	8.92	23.20	10.2350	9.81	2.30	2.97	10.18	9.37	2.70	11.53	3.91	3.38
k_{el} (min^{-1})	0.0064	0.0042	0.0046	0.0064	0.0075	0.0047	0.0059	0.0046	0.0052	0.0054	0.0068	0.0090
$t_{1/2el}$ (min)	108.48	163.92	150.17	109.04	92.17	146.53	116.79	152.32	132.18	129.46	102.30	77.14
MRT (min)	238.61	245.03	195.62	259.95	192.69	225.17	241.72	234.47	209.79	254.24	193.37	194.17
F (%)[d]	–	54.95	20.42									
AUC_t Ratios												
AUC_{brain}/AUC_{plasma}	0.68	1.02	0.97									
AUC_{lung}/AUC_{plasma}	0.67	0.98	1.13									
$AUC_{kidney}/AUC_{plasma}$	1.14	0.99	0.85									

[a] Parameters were estimated using the mean concentration-time profiles obtained from five different animals per time point ($n = 5$). [b] Values expressed in μg/g; [c] Values expressed in μg.min/g; [d] Absolute intranasal bioavailability (F) was calculated based on AUC_{inf} values; AUC_{extrap}, extrapolated area under drug concentration-time curve; AUC_{inf}, area under drug concentration-time curve from time zero to infinity; AUC_t, Area under the concentration time-curve from time zero to the last quantifiable drug concentration; C_{max}, Maximum peak concentration; k_{el}, Apparent elimination rate constant; MRT, Mean residence time; $t_{1/2el}$, Apparent terminal elimination half-life; t_{max}, Time to achieve the maximum peak concentration

Table III Dose-normalized pharmacokinetic parameters of zonisamide in plasma, brain, lung and kidney tissues following its intranasal (IN, 16.7 mg/kg), intravenous (IV, 16.7 mg/kg) and oral (80 mg/kg) administration to mice

Dose-normalized Pharmacokinetic Parameters[a]	Plasma			Brain			Lung			Kidney		
	IV	IN	Oral	IV	IN	Oral	IV	IN	Oral	IV	IN	Oral
C_{max}/Dose (μg/mL or μg/g)/(mg/kg)	0.82	0.60	0.39	0.52	0.41	0.21	0.53	1.06	0.24	1.07	0.55	0.21
AUC_t/Dose (μg.min/mL or μg.min/g)/(mg/kg)	237	110	47.7	162	112	46.1	161	107	53.9	270	141	40.6
AUC_{inf}/Dose (μg.min/mL or μg.min/g)/(mg/kg)	260	143	53.1	180	115	47.6	177	119	55.4	306	147	42.0

[a] Parameters were estimated using the mean concentration-time profiles obtained from five different animals per time point ($n = 5$). AUC_{inf}, Area under the concentration time-curve from time zero to infinite normalized per administered dose; AUC_t, Area under the concentration time-curve from time zero to the last quantifiable drug concentration; C_{max}, Maximum peak concentration

versus 8.93 μg/g). Notwithstanding, when considering lung exposure given by AUC_t and AUC_t/dose, the IV route exhibited higher values [2680.70 μg.min/g and 160.52 (μg/g)/(mg/kg)] than IN route [1794.50 μg.min/g and 107.46 (μg/g)/(mg/kg)], while the oral route stood out as the one with the lowest value of AUC_t/dose [53.95 (μg/g)/(mg/kg), Table III]. The faster C_{max} attainment coupled to the lower exposure observed after IN administration are corroborated by the ratios depicted in Fig. 6B. Accordingly, at 5 min post-administration, the lung-to-plasma ratio observed after IN instillation was almost 10-fold of those observed after the classical administration routes. These statistical differences were readily minimized from the 15 min post-dosing time, even though the evolution of ratios has been very distinct from IV and oral administration, suggesting that a fraction of zonisamide directly reaches the lung. Indeed, the DTE% was 144.47%. For these reasons, the viability of Calu-3 cells was assessed in vitro after exposure to zonisamide, as discussed in **section "In Vitro Cell Viability Studies"**.

With respect to zonisamide concentrations found in kidney tissue up to 480 min (Fig. 4D), the IN route displayed the lowest values. Indeed, at all collected time-points, the concentrations were always inferior to those obtained with IV injection, as well as the C_{max} and AUC values (Table III). Complementarily, when analyzing normalized concentration-time profiles (Fig. 5D), both IN and oral administrations showed decreased concentrations in kidney relatively to IV injection. However, the concentrations found after IN were slightly higher than those obtained by oral route, with statistical differences at 15 min. These findings are further

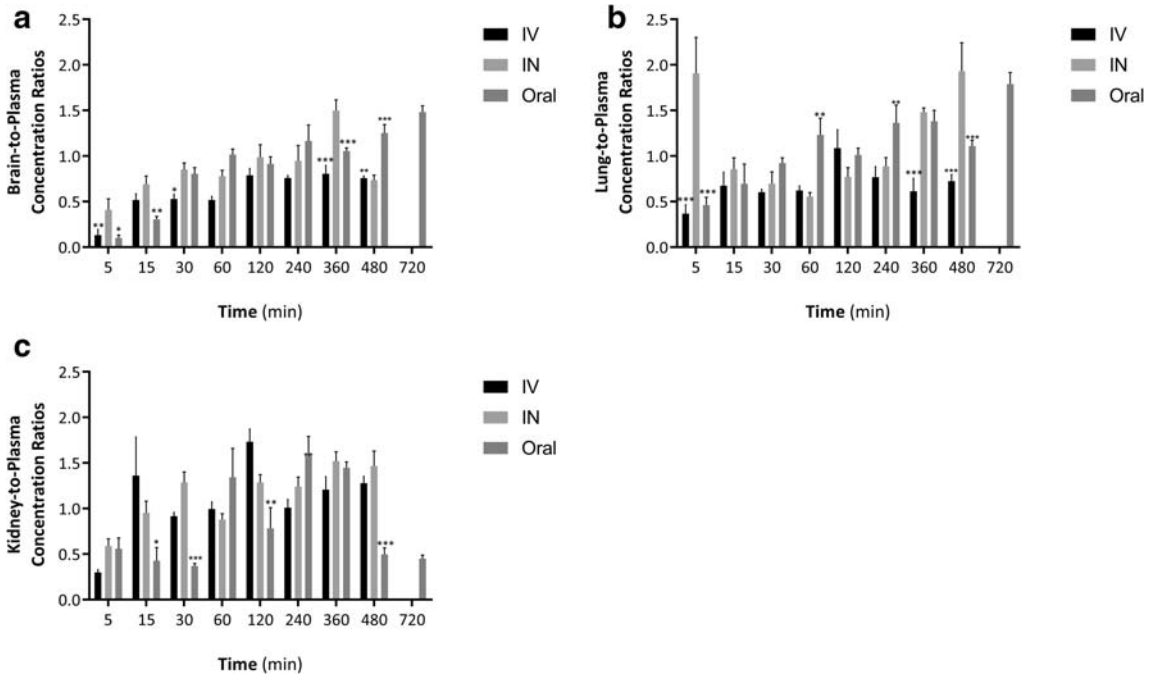

Fig. 6 – Tissue-to-plasma concentration ratios of zonisamide at 5, 15, 30, 60, 120, 240, 360, 480 and 720 min after drug administration by intranasal (IN), intravenous (IV) or oral route. **A** represents the variation of brain-to-plasma concentration ratios versus time; **B** represents the variation of lung-to-plasma concentration ratios versus time and **C** represents the variation of kidney-to-plasma concentration ratios versus time. Statistical differences are in relation to the IV administration route as follows: *$p < 0.05$, **$p < 0.01$, ***$p < 0.001$ assessed by two-way ANOVA followed by Dunnett's multiple comparison test

supported by the fact that zonisamide renal exposure (given by C_{max}/dose and AUC/dose) was approximately half of that observed after IV injection, but twice of that found after oral administration (Table III). Nonetheless, after IN instillation, C_{max} was attained much latter (t_{max} = 120 min) than after IV (t_{max} = 15 min) or oral (t_{max} = 60 min) administrations (Table II). In addition, it is also important to emphasize that the DTE observed for zonisamide in the kidney after IN administration was 1.12. This was the lowest value compared to the other tissues, suggesting that zonisamide has a decreased ability to accumulate in the kidney. Consistently, zonisamide remained in the kidney for the shortest period when intranasally administered (193.37 min versus 194.14 min and 254.24 min after oral and IV routes, respectively, Table II). The kidney-to-plasma ratios observed for IN zonisamide are very similar to those registered with IV and oral formulations, occasionally presenting statistically significant differences with oral zonisamide at 30, 120 and 480 min post-administration (Fig. 6C).

DISCUSSION

Aiming at formulating a successful and original nose-to-brain drug delivery system, but keeping it simple and achievable, the experimental design was optimized in order to warrant that zonisamide was administered in olfactory mucosa of the respiratory mucosa. The accessibility to these regions is rather difficult in mice, particularly due to their small dimensions. Although drug administration into the nose is often performed using a pipette or a polyethylene tube attached to a microsyringe/micropipette (41,42), herein we preferred to use the MicroSprayer® Aerosolizer and to load zonisamide in an in situ-gelling hydrogel, the Pluronic F-127 vehicle. This choice was based on our recent studies that demonstrated that almost 50% of levetiracetam undergoes direct nose-to-brain delivery after its nasal administration (23,41–45). Nonetheless, to increase in situ-gelling properties and mucoadhesion, Carbopol® 974P and Noveon® Polycarbophil polymers were herein investigated and subjected to cellular viability tests to select the safest one for IN administration to mice. The results found in the RPMI 2640 cell line for zonisamide and the four formulations (empty and drug-loaded) are depicted in Figs. 2 and 3. Accordingly, the thermoreversible mucoadhesive gel prepared with Carbopol® 974P (0.2%) plus Pluronic F-127 (18%) exhibited higher values of RPMI-2650 cells viability in relation to the control and the other tested gel, and therefore it was selected to incorporate and deliver zonisamide at the dose of 16.7 mg/kg by IN route.

Although zonisamide is only currently marketed in oral dosage forms, IV route was herein used as control because the absolute oral bioavailability of zonisamide was only 20.42% in mice (Table II), unlike in humans, where it ranges 60–100% (46,47). Moreover, when assessing the potential of a new route of administration, IV administration is recommended to be used for comparison, since intestinal absorption is avoided, decreasing the variability that may occur during incorporation. Importantly, the blood-mediated zonisamide delivery into the CNS after drug nasal instillation is estimated by IV injection and, consequently, the fraction of the drug directly transported from nose-to-brain is more accurately discriminated. Nevertheless, the pharmacokinetics of oral zonisamide was also assessed in an attempt to investigate whether systemic and brain exposures after nasal administration were within safe therapeutic ranges. This is determinant, because DTE and DTP are limited when used alone and are associated to high variability. Therefore, the orally administered dose was defined to achieve plasma concentrations within human therapeutic range of 10–40 μg/mL (46,47). It was established at 80 mg/kg since plasma concentrations were within it up to 120 min post-dosing (Fig. 4). Given that the oral dose was more than four-times higher than the nasal and IV ones (16.7 mg/kg), concentrations reached in plasma, brain, lung and kidney were dose-normalized (Fig. 5), as well as the pharmacokinetic parameters which directly depended on administered doses (C_{max} and AUC, Table III). Only applying this strategy, could oral results be compared with the remaining ones.

Pharmacokinetic results revealed that, similarly to IV injection, the IN administration of zonisamide nasal gel allowed zonisamide to be quickly absorbed into the bloodstream (t_{max} of 5 min) while oral route required 15 min to attain t_{max}. On the other hand, zonisamide concentrations attained in plasma after IN instillation were considerably lower than those observed after IV injection (Fig. 4A), limiting systemic drug exposure (given by C_{max}, AUC_t and AUC_{inf}). This was supported by the absolute IN bioavailability of only 54.95% (Table II). Although it is undeniable that a significant amount of zonisamide was not absorbed through nasal respiratory epithelium to bloodstream, the almost overlapping time course of plasma and brain concentrations after both routes of administration suggest that a fraction of the drug was absorbed to the systemic circulation, attaining the CNS after crossing the BBB. Nevertheless, bearing in mind that the present work intended to promote a direct nose-to-brain delivery of zonisamide, the absolute bioavailability of only 54.95% may not hamper the drug from targeting the CNS. Moreover, it is expected to be advantageous, as fewer systemic side effects are probable to occur after IN administration. Indeed, as discussed in **section "Pharmacokinetics of Zonisamide"**, brain concentrations of IN zonisamide at 5.00 min were 8.66-fold higher than after IV injection and DTE was 149.54%, suggesting that a direct transport of zonisamide occurs from nasal mucosa to the brain through the olfactory and/or trigeminal nerve pathways. DTE represents

the ratio between brain and plasma concentrations after IN administration in comparison to IV injection. According to Fatouh et al. (36) and Pires et al. (40), values higher than 1.0 indicate more efficient brain targeting following IN administration. Furthermore, the calculated DTP for zonisamide IN gel highlights that 33.13% of the drug that reaches the brain attains it through direct nose-to-brain mechanisms, circumventing the BBB. The results found for the DTE and DTP, together with the pharmacokinetic behavior of zonisamide in plasma and brain after IN administration comparatively to classical routes are the base for the development of new mathematical pharmacokinetic/pharmacodynamic models as Ruigrok and Lange suggest (48). Moreover, these findings are of huge clinical relevance, because 30–40% of medicated epileptic patients develop drug-resistant epilepsy, which has been associated, among other mechanisms, to the overexpression of efflux transporters located in peripheral organs and endothelial cells of BBB. Consequently, the available concentrations to reach the CNS are reduced (49,50). Therefore, by circumventing BBB and enabling a direct nose-to-brain transport of zonisamide, the original strategy herein exploited may become successful for the treatment of drug-resistant epilepsy.

Bearing in mind that IV zonisamide is not available in clinical practice, oral administration was also investigated in order to compare the ability of IN administration to deliver higher zonisamide concentrations into the brain, without compromising systemic safety. Thus, the relative bioavailability of nasal thermoreversible gel was 269.08%, suggesting that the concentration of systemically absorbed drug through the respiratory epithelium is more than twice of that absorbed at the intestinal level. These results reinforce that the nasal first-passage effect is less relevant than the intestinal and hepatic pre-systemic effects that occur after oral administration. As explained in introduction, zonisamide is highly metabolized in humans by CYP3A4 and CYP2C19 (18,20) which is one of the major drawbacks of the current oral forms available in clinical practice (14). Applying the novel nose-to-brain strategy, drug-drug interactions and inter-individual pharmacokinetic variability are expected to decrease or become negligible.

In addition, it is noteworthy that the brain concentrations of zonisamide after oral administration are considerably higher (Fig. 4B). However, when dose-normalized concentrations are plotted against time administration (Fig. 5B), it becomes clear that these differences result from the higher orally administered dose. Indeed, IN and IV routes exhibit dose-normalized C_{max} and AUC that are more than twice of those of oral administration (Table III). In addition, IN route has the highest $AUC_{tbrain}/AUC_{tplasma}$ ratio (1.02 versus 0.68 for IV and 0.98 for oral administrations, Table II), confirming that the IN route allows a higher brain exposure, despite lower systemic drug exposure. Interestingly, since zonisamide was quantified only up to 8 h and the intracellular nose-to-brain transport implies 1.5–6 h through the olfactory route and 17–56 h through the trigeminal nerve (28, 51), it can be hypothesized that zonisamide directly attained the brain through the olfactory pathway. Despite the above conclusions, specific biodistribution and pharmacodynamic studies should be carried out in the future to clarify the issue.

In order to assess whether IN administration could compromise drug safety at pulmonary level, the pharmacokinetics of zonisamide in lungs was compared after administration by the three routes. It was clearly observed that lung concentrations of zonisamide at 5 min post-dosing were considerably superior after IN administration than intravenously (17.66 ± 2.651 and 3.33 ± 1.004 μg/g, respectively; $p = 0.007$) (Fig. 4C). Nonetheless, at the remaining time-points, concentrations were always lower after IN instillation (Fig. 4C). In addition, lung exposure given by AUC was lower for IN administration than for IV route (Table II), suggesting that pulmonary safety is expected to be maintained. These data are corroborated by the inferior value of $AUC_{tlung}/AUC_{tplasma}$ observed with IN instillation than oral administration (Table II and Fig. 6B). Additionally, zonisamide did not compromise the viability of Calu-3 cells after 24 h of exposure at concentrations between 1.0 and 100 μM (Fig. 2), which include the concentrations found during preclinical in vivo investigation herein performed.

Finally, zonisamide pharmacokinetics was also assessed in kidney, particularly due to the its most relevant side effect, i.e. renal lithiasis. Higher zonisamide concentrations in kidney were found after IV injection than those observed with the thermoreversible gel (Fig. 4D), substantiating that the drug has enhanced renal exposure after IV injection. Comparing with oral route, kidney exposure (given by C_{max} and AUC_t and AUC_{inf}) after dose-normalization was higher for intranasal route (Table III). Nevertheless, nasal route is expected to require lower doses than the oral, since the first-passage effect in the nasal cavity is less than in the intestine.

In conclusion, the present study demonstrated that the IN administration of zonisamide allowed a faster drug targeted-uptake into the brain, in relation to the IV injection. Moreover, systemic absorption through respiratory epithelium was approximately 50% of IV route, which is considered advantageous, since fewer systemic side effects are expected to occur. The IN administration of zonisamide was also compared to the oral route, corroborating the obtained results and highlighting that drug exposure in lungs and kidneys are comparable for the three administration routes, thereby prospecting very similar pharmacological responses at those levels. Thus, the novel nose-to-brain strategy herein investigated for the first time seems to be beneficial to directly deliver the drug into the CNS, representing a suitable and promising alternative route for zonisamide administration, not only for chronic treatment of epilepsy or Parkinson's disease but also in acute emergency situations, such as *status epilepticus*. In addition

to this, zonisamide is currently marketed only in oral forms, requiring novel formulations that can be used in acute situations. From this perspective, the discussed in vitro/in vivo results support that the aforementioned clinical needs can be met by resorting to the applied nose-to-brain strategy. It will be an economical strategy, applicable to patients with physiological or pathophysiological swallowing restrictions (pediatrics, geriatrics, among others). Importantly, the quantitative pharmacokinetic data herein obtained for the three administration routes will be also of utmost importance to develop pharmacokinetic/pharmacodynamic mathematical models that can be, then, scaled to humans.

ACKNOWLEDGMENTS AND DISCLOSURES

The authors acknowledge to Fundo Europeu de Desenvolvimento Regional (FEDER) funds through Portugal 2020 in the scope of the Operational Programme for Competitiveness and Internationalisation, and Fundação para a Ciência e Tecnologia (FCT) I.P./MCTES, Portuguese Agency for Scientific Research, through national funds (PIDDAC) within the scope of the research project CENTRO-01-0145-FEDER-03075 and POCI-01-0145-FEDER-030478.

REFERENCES

1. Park KM, Lee BI, Shin KJ, Ha SY, Park J, Kim SE, et al. Efficacy, tolerability, and blood concentration of zonisamide in daily clinical practice. J Clin Neurosci. 2019;61:44–7.
2. Sano H, Nambu A. The effects of zonisamide on L-DOPA-induced dyskinesia in Parkinson's disease model mice. Neurochem Int. 2019;124:171–80.
3. Iwaki H, Tagawa M, Iwasaki K, Kawakami K, Nomoto M. Comparison of zonisamide with non-levodopa, anti-Parkinson's disease drugs in the incidence of Parkinson's disease-relevant symptoms. J Neurol Sci. 2019;402:145–52.
4. Nishijima H, Miki Y, Ueno S, Tomiyama M. Zonisamide enhances motor effects of levodopa, not of Apomorphine, in a rat model of Parkinson's disease. Parkinson's Dis. 2018;2018:8626783.
5. Limmer AL, Holland LC, Loftus BD. Zonisamide for cluster headache prophylaxis: a case series. Headache. 2019;59(6):924–9.
6. Martinez-Avila JC, Garcia Bartolome A, Garcia I, Dapia I, Tong HY, Diaz L, et al. Pharmacometabolomics applied to zonisamide pharmacokinetic parameter prediction. Metabol: Off J Metabol Soc. 2018;14(5):70.
7. Kanner AM, Ashman E, Gloss D, Harden C, Bourgeois B, Bautista JF, et al. Practice guideline update summary: efficacy and tolerability of the new antiepileptic drugs I: treatment of new-onset epilepsy: report of the guideline development, dissemination, and implementation Subcommittee of the American Academy of neurology and the American Epilepsy Society. Neurology. 2018;91(2):74–81.
8. Hershey LA, Coleman-Jackson R. Pharmacological Management of Dementia with Lewy bodies. Drugs Aging. 2019;36(4):309–19.
9. Sano H, Murata M, Nambu A. Zonisamide reduces nigrostriatal dopaminergic neurodegeneration in a mouse genetic model of Parkinson's disease. J Neurochem. 2015;134(2):371–81.
10. Reimers A, Ljung H. An evaluation of zonisamide, including its long-term efficacy, for the treatment of focal epilepsy. Expert Opin Pharmacother. 2019;20(8):909–15.
11. Kubota M, Nishi-Nagase M, Sakakihara Y, Noma S, Nakamoto M, Kawaguchi H, et al. Zonisamide - induced urinary lithiasis in patients with intractable epilepsy. Brain Dev. 2000;22(4):230–3.
12. Jion YI, Raff A, Grosberg BM, Evans RW. The risk and management of kidney stones from the use of topiramate and zonisamide in migraine and idiopathic intracranial hypertension. Headache. 2015;55(1):161–6.
13. Bejjanki H, Bird V, Ruchi R. Letter to the editor regarding the manuscript "efficacy, tolerability, and blood concentration of zonisamide in daily clinical practice". J Clin Neurosci: Off J Neurosurg Soc Aust. 2019;63:283.
14. Sills G, Brodie M. Pharmacokinetics and drug interactions with zonisamide. Epilepsia. 2007;48(3):435–41.
15. McCleane G. Pharmacological management of neuropathic pain. CNS drugs. 2003;17(14):1031–43.
16. Levy RH, Ragueneau-Majlessi I, Garnett WR, Schmerler M, Rosenfeld W, Shah J, et al. Lack of a clinically significant effect of zonisamide on phenytoin steady-state pharmacokinetics in patients with epilepsy. J Clin Pharmacol. 2004;44(11):1230–4.
17. Frampton JE, Scott LJ. Zonisamide: a review of its use in the management of partial seizures in epilepsy. CNS drugs. 2005;19(4):347–67.
18. Nakasa H, Nakamura H, Ono S, Tsutsui M, Kiuchi M, Ohmori S, et al. Prediction of drug-drug interactions of zonisamide metabolism in humans from in vitro data. Eur J Clin Pharmacol. 1998;54(2):177–83.
19. Loscher W, Klotz U, Zimprich F, Schmidt D. The clinical impact of pharmacogenetics on the treatment of epilepsy. Epilepsia. 2009;50(1):1–23.
20. Saruwatari J, Ishitsu T, Nakagawa K. Update on the Genetic Polymorphisms of Drug-Metabolizing Enzymes in Antiepileptic Drug Therapy. Pharmaceuticals (Basel, Switzerland). 2010;3(8):2709–32.
21. Goto S, Seo T, Murata T, Nakada N, Ueda N, Ishitsu T, et al. Population estimation of the effects of cytochrome P450 2C9 and 2C19 polymorphisms on phenobarbital clearance in Japanese. Ther Drug Monit. 2007;29(1):118–21.
22. Vitorino C, Silva S, Bicker J, Falcao A, Fortuna A. Antidepressants and nose-to-brain delivery: drivers, restraints, opportunities and challenges. Drug Discov Today. 2019;24(9):1911–23.
23. Goncalves J, Bicker J, Gouveia F, Liberal J, Oliveira RC, Alves G, et al. Nose-to-brain delivery of levetiracetam after intranasal administration to mice. Int J Pharm. 2019;564:329–39.
24. Sabir F, Ismail R, Csoka I. Nose-to-brain delivery of antiglioblastoma drugs embedded into lipid nanocarrier systems: status quo and outlook. Drug Discov Today. 2019.
25. Martins PP, Smyth HDC, Cui Z. Strategies to facilitate or block nose-to-brain drug delivery. Int J Pharm. 2019;570:118635.
26. Wang Z, Xiong G, Tsang WC, Schatzlein AG, Uchegbu IF. Nose-to-brain delivery. J Pharmacol Exp Ther. 2019;370(3):593–601.
27. Agrawal M, Saraf S, Saraf S, Antimisiaris SG, Chougule MB, Shoyele SA, et al. Nose-to-brain drug delivery: an update on clinical challenges and progress towards approval of anti-Alzheimer drugs. J Control Rel: Off J Control Rel Soc. 2018;281:139–77.
28. Crowe TP, Greenlee MHW, Kanthasamy AG, Hsu WH. Mechanism of intranasal drug delivery directly to the brain. Life Sci. 2018;195:44–52.
29. Romanelli MC, Gelardi M, Fiorella ML, Tattoli L, Di Vella G, Solarino B. Nasal ciliary motility: a new tool in estimating the time of death. Int J Legal Med. 2012;126(3):427–33.
30. O'Brien J, Wilson I, Orton T, Pognan F. Investigation of the Alamar blue (resazurin) fluorescent dye for the assessment of mammalian cell cytotoxicity. Eur J Biochem. 2000;267(17):5421–6.

31. Goncalves J, Alves G, Bicker J, Falcao A, Fortuna A. Development and full validation of an innovative HPLC-diode array detection technique to simultaneously quantify lacosamide, levetiracetam and zonisamide in human plasma. Bioanalysis. 2018;10(8):541–57.
32. EMA. Guideline on bioanalytical method validation. 2012.
33. EMA. ICH Harmonised Guideline M10 on Bioanalytical Method Validation - step 2b. 2019.
34. FDA. Bioanalytical Method Validation Guidance for Industry. 2018.
35. Raval N, Barai P, Acharya N, Acharya S. Fabrication of peptide-linked albumin nanoconstructs for receptor-mediated delivery of asiatic acid to the brain as a preventive measure in cognitive impairment: optimization, in-vitro and in-vivo evaluation. Artificial cells, nanomedicine, and biotechnology. 2018;46(sup3):S832-s46.
36. Fatouh AM, Elshafeey AH, Abdelbary A. Agomelatine-based in situ gels for brain targeting via the nasal route: statistical optimization, in vitro, and in vivo evaluation. Drug Del. 2017;24(1):1077–85.
37. Fatouh AM, Elshafeey AH, Abdelbary A. Intranasal agomelatine solid lipid nanoparticles to enhance brain delivery: formulation, optimization and in vivo pharmacokinetics. Drug Des, Devel Ther. 2017;11:1815–25.
38. Katare YK, Piazza JE, Bhandari J, Daya RP, Akilan K, Simpson MJ, et al. Intranasal delivery of antipsychotic drugs. Schizophr Res. 2017;184:2–13.
39. Kozlovskaya L, Abou-Kaoud M, Stepensky D. Quantitative analysis of drug delivery to the brain via nasal route. J Control Rel: Off J Control Rel Soc. 2014;189:133–40.
40. Pires PC, Santos AO. Nanosystems in nose-to-brain drug delivery: a review of non-clinical brain targeting studies. J Control Rel: Off J Control Rel Soc. 2018;270:89–100.
41. Fortuna A, Alves G, Serralheiro A, Sousa J, Falcao A. Intranasal delivery of systemic-acting drugs: small-molecules and biomacromolecules. Eur J Pharm Biopharm. 2014;88(1):8–27.
42. Serralheiro A, Alves G, Fortuna A, Falcao A. Direct nose-to-brain delivery of lamotrigine following intranasal administration to mice. Int J Pharm. 2015;490(1–2):39–46.
43. Sousa J, Alves G. Intranasal Del Topically-Acting Levofloxacin Rats: Proof-of-Conc Pharmacok Study. 2017;34(11):2260–9.
44. Cunha-Filho MS, Alvarez-Lorenzo C, Martinez-Pacheco R, Landin M. Temperature-sensitive gels for intratumoral delivery of beta-lapachone: effect of cyclodextrins and ethanol. TheScientificWorldJournal. 2012;2012:126723.
45. Zahir-Jouzdani F, Wolf JD, Atyabi F, Bernkop-Schnurch A. In situ gelling and mucoadhesive polymers: why do they need each other? Expert Opin Del. 2018;15(10):1007–19.
46. Hiemke C, Bergemann N, Clement HW, Conca A, Deckert J, Domschke K, et al. Consensus guidelines for therapeutic drug monitoring in Neuropsychopharmacology: update 2017. Pharmacopsychiatry. 2018;51(1–02):e1.
47. Jacob S, Nair AB. An updated overview on therapeutic drug monitoring of recent antiepileptic drugs. Drugs in R&D. 2016;16(4):303–16.
48. Ruigrok MJ, de Lange EC. Emerging insights for translational pharmacokinetic and pharmacokinetic-Pharmacodynamic studies: towards prediction of nose-to-brain transport in humans. AAPS J. 2015;17(3):493–505.
49. Kwan P, Arzimanoglou A, Berg AT, Brodie MJ, Allen Hauser W, Mathern G, et al. Definition of drug resistant epilepsy: consensus proposal by the ad hoc task force of the ILAE commission on therapeutic strategies. Epilepsia. 2010;51(6):1069–77.
50. Leandro K, Bicker J, Alves G, Falcao A, Fortuna A. ABC transporters in drug-resistant epilepsy: mechanisms of upregulation and therapeutic approaches. Pharmacol Res. 2019;144:357–76.
51. Lochhead JJ, Wolak DJ, Pizzo ME, Thorne RG. Rapid transport within cerebral perivascular spaces underlies widespread tracer distribution in the brain after intranasal administration. J Cereb Blood Flow Metab: Off J Int Soc Cereb Blood Flow Metab. 2015;35(3):371–81.